A New Method for Simultaneous Determination of Anisotropic Thermal Conductivities Based on Two-Dimensional Analysis

2001 Jpn. J. Appl. Phys. 40 388

(http://iopscience.iop.org/1347-4065/40/1R/388)

Jpn. J. Appl. Phys. Vol. 40 (2001) pp. 388–392
Part 1, No. 1, January 2001

A New Method for Simultaneous Determination of Anisotropic Thermal Conductivities Based on Two-Dimensional Analysis

Hiroyuki FUJISHIRO, Tatsuya OKAMOTO, Manabu IKEBE and Koichi HIROSE
Faculty of Engineering, Iwate University, 4-3-5 Ueda, Morioka 020-8551, Japan

(Received May 31, 2000; revised manuscript received August 28, 2000; accepted for publication October 12, 2000)

A new experimental setup and analysis method for simultaneous determination of the anisotropic thermal conductivities (κ_x, κ_y) is proposed for materials with uniaxial anisotropy or a layered structure. By applying heat power diagonally through the sample from a heater to a cold finger, temperature differences (ΔT_x, ΔT_y) along the two directions were monitored. The monitored temperature differences were compared with $\Delta T'_x$ and $\Delta T'_y$, which were calculated by solving a two-dimensional heat diffusion equation. Calculations were repeated until $\Delta T'_x$ and $\Delta T'_y$ agreed with ΔT_x and ΔT_y, to determine κ_x and κ_y. This technique was applied to a carbon-fiber-reinforced plastic (CFRP) from 40 K to 200 K and a satisfactory agreement was achieved with the κ_x and κ_y values and those determined from independent measurements of κ_x and κ_y.

KEYWORDS: anisotropic materials, anisotropic thermal conductivity, low temperature, heat diffusion equation, identical experimental setup

1. Introduction

In the field of low-temperature physics and cryogenic engineering, many structurally anisotropic materials [*e.g.* single crystals of high-T_c superconductors and fiber-reinforced plastics (FRPs)] are used as functional and constructive materials. It is very important to investigate their anisotropic natures in terms of their mechanical, electrical and thermal transport properties. The thermal conductivity $\kappa(T)$ is a valuable parameter for practical use such as in the design of cryostats and power leads for superconducting magnets.[1] As shown in Fig. 1(a), $\kappa(T)$ is usually measured by a one-dimensional (1D) steady-state heat flow method using a long rectangular-shaped sample, which is based on the relation $\kappa = (Q/\Delta T)(L/S)$,[2] where Q is the applied heat power, S the cross section of a sample, and ΔT and L the temperature difference and distance between thermometers, respectively. For anisotropic materials, anisotropic κ values (*e.g.* κ_x, κ_y, κ_z) are measured in separate experimental setups using long rectangular-shaped samples cut along each direction. In layered compounds, for example, only a plate-like single crystal can be obtained and it is often difficult to prepare long samples to realize a homogeneous 1D heat flow for perpendicular conductivity ($\kappa_\perp$) measurement. Figure 1(b) shows a conventional experimental setup for $\kappa_\perp$ measurement perpendicular to the sample face of a plate-like material.[3] A sapphire plate with a higher thermal conductivity is attached to the sample face and a heater is adhered to the sapphire plate. Because of the short distance L of the sample, the thermocouples cannot be attached directly to the sample and temperatures have to be measured on both the sapphire plate and the cold finger. In this case, which is referred to as a thermally two-terminal method, the contact thermal resistivity W_c between the sample and the sapphire (the cold finger) significantly influences the ΔT measurement. Furthermore, the wide contact area between the sapphire plate (or the cold finger) and the sample may prevent homogeneous 1D heat flow because of the inhomogeneity of W_c in the contact area. Therefore, it is desirable to measure $\kappa_\perp(T)$ without the influence of W_c.

In this paper, we propose a new method to enable simultaneous determination of the anisotropic thermal conductivities (κ_x, κ_y) in samples having two-dimensional (2D) anisotropy using an identical experimental setup which is free from the influence of W_c. This method has been applied to a carbon-fiber-reinforced plastic (CFRP) from 40 K to 200 K and was verified to obtain κ_x and κ_y with high precision.

2. Experimental Procedure

Figure 2 shows a schematic view of the experimental setup around the sample. A rectangular sample with uniaxial anisotropy is situated parallel to the x- and y-axes. The sample is thermally connected to a heater and a cold finger and

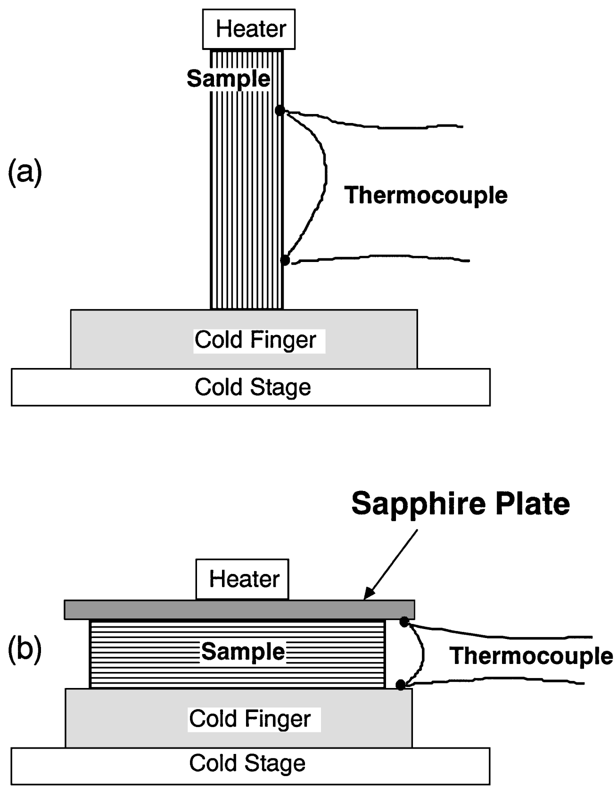

Fig. 1. (a) Conventional experimental setup for $\kappa(T)$ measurement by a steady-state heat flow method using a long sample. (b) Conventional experimental setup for the perpendicular conductivity ($\kappa_\perp$) measurement. A sapphire plate is attached to the sample face and a heater is adhered to the sapphire plate.

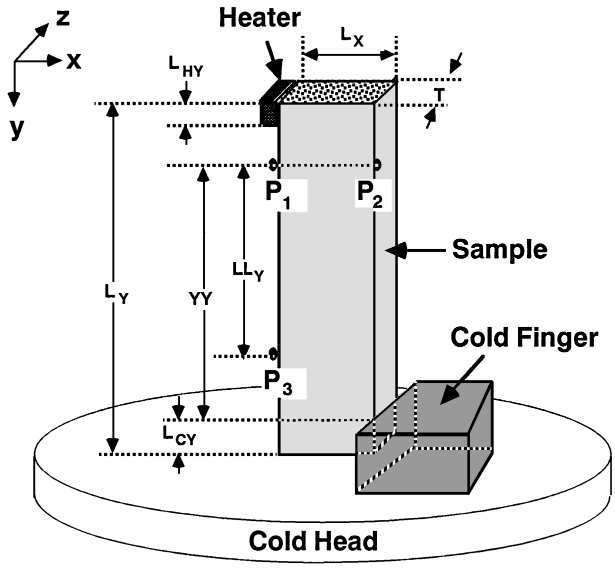

Fig. 2. Schematic diagram of the new experimental setup around the sample in this study.

heat power Q is applied diagonally through the sample. In this situation, temperatures at three measuring points, P_1, P_2 and P_3, increase due to heat flow, and the temperature rise (ΔT_1, ΔT_2, ΔT_3) at each point is determined by thermal conductivities (κ_x, κ_y) along the x- and y-directions and the applied heat power Q. The temperature differences, $\Delta T_x = \Delta T_1 - \Delta T_2$ and $\Delta T_y = \Delta T_1 - \Delta T_3$, also change depending on the magnitudes of κ_x, κ_y and Q. The measured temperature differences (ΔT_x and ΔT_y) after the application of heat power are compared with calculated ones ($\Delta T'_x$ and $\Delta T'_y$) obtained by solving a two-dimensional heat diffusion equation including different pairs of anisotropic thermal conductivities (κ'_x and κ'_y). This procedure is continued until $\Delta T_x = \Delta T'_x$ and $\Delta T_y = \Delta T'_y$ are achieved at each measuring temperature and the thermal conductivities along the two directions, $\kappa_x(T)$ and $\kappa_y(T)$, can be determined.

Table I shows sizes and lengths in the experimental setup shown in Fig. 2. The measured sample was a CFRP with a fiber volume fraction of $V_f = 0.6$. The high-κ carbon fiber was aligned along the y-direction. The sample size was $5.7 \times 5.5 \times 30\,\text{mm}^3$ in the x-, z- and y-directions. A Gifford-McMahon (GM) cycle helium refrigerator was used as a cryostat and a copper cold finger was attached to the cold head of the GM refrigerator.[4)] The sample was adhered to both a metal film resistance heater ($1\,\text{k}\Omega$; $2.0 \times 5.5 \times 2.5\,\text{mm}^3$) and the copper cold finger using Ag paste. AuFe(0.07 at.%)-chromel thermocouples with a $76\,\mu$m ϕ were used to measure temperatures at the three positions (P_1, P_2 and P_3). The detection limit of the temperature difference ΔT was $\approx$0.005 K. The measurement was performed from 40 to 200 K. The sample was enclosed by a radiation shield of Ni-plated copper which was thermally anchored to the cold head. The sample chamber was evacuated to $<1 \times 10^{-5}$ Torr by an oil diffusion pump to prevent heat convection and conduction by remanent gas. After heat power Q was applied to the CFRP sample and a steady heat-flow state was realized, the temperature differences ΔT_x and ΔT_y were measured.

3. Numerical Solution of 2D Heat Diffusion Equation

In the case that heat power Q is applied diagonally to a uniaxially anisotropic material using the experimental setup shown in Fig. 2, the time dependence of the temperature variation at a certain position $T(x, y, t)$ can be given by solving the following 2D heat diffusion equation,[5)]

$$\frac{\partial T}{\partial t} = \alpha_x \frac{\partial^2 T}{\partial x^2} + \alpha_y \frac{\partial^2 T}{\partial y^2} = \frac{\kappa_x}{dC}\frac{\partial^2 T}{\partial x^2} + \frac{\kappa_y}{dC}\frac{\partial^2 T}{\partial y^2}, \tag{1}$$

where α_x and α_y (cm^2/s) are the thermal diffusivities along the x- and y-directions, respectively, d (g/cm^3) is the mass density and C (J/cm^{3}K) is the specific heat per volume of the sample. The sample lengths L_X and L_Y and time t are divided into equal intervals Δx, Δy and Δt, respectively, so that the x-y-t space is covered by a grid of rectangles. Equation (1) can be represented by the following finite-difference solution using an explicit method,

$$\begin{aligned}\frac{T(i,j,t+\Delta t) - T(i,j,t)}{\Delta t} = {} & \frac{\kappa_x}{dC}\frac{T(i+1,j,t) - 2T(i,j,t) + T(i-1,j,t)}{\Delta x^2} \\ & + \frac{\kappa_y}{dC}\frac{T(i,j+1,t) - 2T(i,j,t) + T(i,j-1,t)}{\Delta y^2},\end{aligned} \tag{2}$$

where $T(i, j, t)$ is a temperature at a grid point (i, j) at time t with i and j being integers, and $T(i, j, t + \Delta t)$ is a temperature at the point (i, j) after a time interval Δt. It is to be noted that the spacial coordinates of the grid point (i, j) are $x = i \times \Delta x$ and $y = j \times \Delta y$, respectively. We can rearrange eq. (2) as follows:

$$\begin{aligned}T(i,j,t+\Delta t) = {} & T(i,j,t) + \frac{\kappa_x}{dC}\frac{\Delta t}{\Delta x^2}\{T(i+1,j,t) - 2T(i,j,t) + T(i-1,j,t)\} \\ & + \frac{\kappa_y}{dC}\frac{\Delta t}{\Delta y^2}\{T(i,j+1,t) - 2T(i,j,t) + T(i,j-1,t)\}.\end{aligned} \tag{3}$$

Thus, the unknown temperature $T(i, j, t + \Delta t)$ at the point (i, j) after the time interval Δt can be represented in terms of the five known temperatures, $T(i+1, j, t)$, $T(i, j, t)$, $T(i-1, j, t)$, $T(i, j+1, t)$ and $T(i, j-1, t)$. In order to illuminate the principle and procedure of the proposed method, we present typical results of numerical solutions of eq. (3). The temperature rise at a given point i, ΔT_i, was normalized by the maximum temperature difference in the sample, $T_H - T_C$, where T_H is the temperature at the sample surface area where the heater is attached and T_C is the temperature at the sample surface area where the cold finger is attached. This normalized temperature rise was then denoted $\Delta T''_i$. Accord-

Table I. Meanings of symbols and lengths in experimental setup shown in Fig. 2.

Symbol	Length (mm)	Remarks
L_Y	30.0	length of the sample along the y-direction
L_X	5.7	distance between P_1 and P_2 (length of the sample along the x-direction)
T	5.5	length of the sample along the z-direction
LL_Y	12.8	distance between P_1 and P_3
L_{CY}	6.4	contact length with cold finger (y-direction)
L_{HY}	2.5	contact length with heater (y-direction)
YY	20.1	distance between P_1 and the upper surface of cold finger

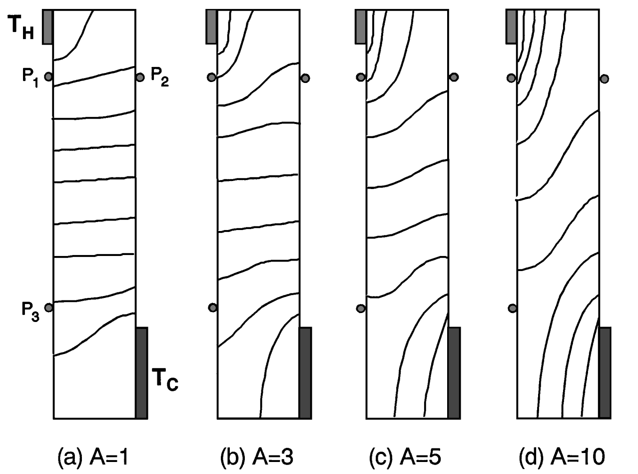

Fig. 3. Calculated isothermal lines (every $\Delta T'' = 0.1$) in the sample for (a) $A(=\kappa_y/\kappa_x) = 1$, (b) $A = 3$, (c) $A = 5$ and (d) $A = 10$. Sample size and the lengths in the experimental setup are set as shown in Table I. Temperature difference $\Delta T''$ is reduced by the maximum temperature difference ΔT_{max} ($=T_H - T_C$) between the temperatures of the sample surfaces at the heater (T_H) and at the cold finger (T_C) (see text).

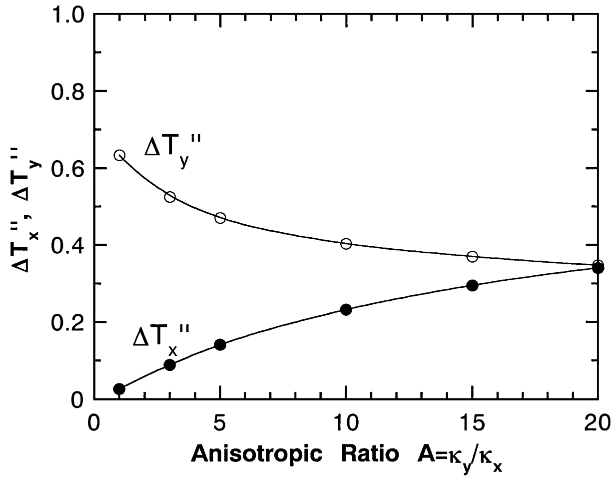

Fig. 4. Calculated normalized temperature differences $\Delta T_x''$ (between P_1 and P_2) and $\Delta T_y''$ (between P_1 and P_3) as a function of the anisotropic thermal conductivity ratio A. $\Delta T_x''$ and $\Delta T_y''$ are normalized by ΔT_{max}.

ingly, the normalized temperature difference between each point of the sample was denoted by $\Delta T_x'' = \Delta T_1'' - \Delta T_2''$ and $\Delta T_y'' = \Delta T_1'' - \Delta T_3''$. A constant heat flow condition was applied to the surface area where the heater is attached and a constant temperature condition was applied to the surface area where the cold finger is attached. An adiabatic condition ($\partial T/\partial x = 0$ or $\partial T/\partial y = 0$) was applied to the other surface areas. The temperature differences $\Delta T_x''$ and $\Delta T_y''$ in the steady heat flow state were calculated confirming the steady values of the calculated temperatures after a sufficient time lapse. The contact thermal resistivities W_c between the sample and the heater and between the sample and the cold finger do not affect $\Delta T_x''$ and $\Delta T_y''$ in the steady state. In the present calculation, Δx, Δy and Δt were set to be 0.025 mm, 0.04 mm and 0.005 s, respectively.

Figure 3 depicts some examples of calculated isothermal lines. The sample sizes and lengths are summarized in Table I. The given dimensions correspond to the experimental setup in the following section. The isotherm lines are drawn at intervals of $\Delta T'' = 0.1$. The thermal conductivity ratio $A = \kappa_y/\kappa_x$ was changed from $A = 1$ in Fig. 3(a) to $A = 10$ in Fig. 3(d). These figures suggest that the measuring position P_1 should be located as close to the heater as possible because the temperature difference between P_1 and P_2 is then very sensitive to the thermal conductivity ratio A.

Figure 4 shows the calculated reduced temperature differences $\Delta T_x''$ and $\Delta T_y''$ as a function of anisotropy ratio A. It can be confirmed that the temperature difference $\Delta T_x''$ increases with increasing the anisotropy ratio A. On the other hand, $\Delta T_y''$ decreases with increasing A. In actual experiments, the temperature differences ΔT_x and ΔT_y measured at each measuring temperature are determined by the heat power Q and the thermal conductivities κ_x and κ_y along the x- and y-axes, respectively. We uniquely determine the κ_x and κ_y values by comparing the measured ΔT_x and ΔT_y with $\Delta T_x'$ and $\Delta T_y'$ (not reduced) which were numerically calculated on the basis of eq. (3). A conceptional view of the present method is presented in the following figure.

Figures 5(a) and 5(b) present the calculated curves of $\Delta T_x'$ and $\Delta T_y'$ as a function of the thermal conductivity κ_y for several fixed κ_x values under a constant applied heat power Q. We discuss the estimation method only in the $\kappa_y > \kappa_x$ ($A > 1$) region. The temperature difference $\Delta T_x'$ increases with increasing κ_y for a fixed κ_x value but decreases with increasing κ_x for a fixed κ_y value. Conversely, $\Delta T_y'$ values decrease with increasing κ_y for a fixed κ_x value and also decrease with increasing κ_x for a fixed κ_y value. In Fig. 5(a), a set of points at which a calculated $\Delta T_x'$ value is equal to a measured ΔT_x value forms a curve parallel to the κ_x-κ_y plane. A similar curve can be also obtained for $\Delta T_y' = \Delta T_y$ in Fig. 5(b). Figure 5(c) schematically shows the projections of both sets of points to the κ_x-κ_y plane. The cross-point of the two projection curves can thus be uniquely obtained and the anisotropic thermal conductivities (κ_x, κ_y) can be determined.

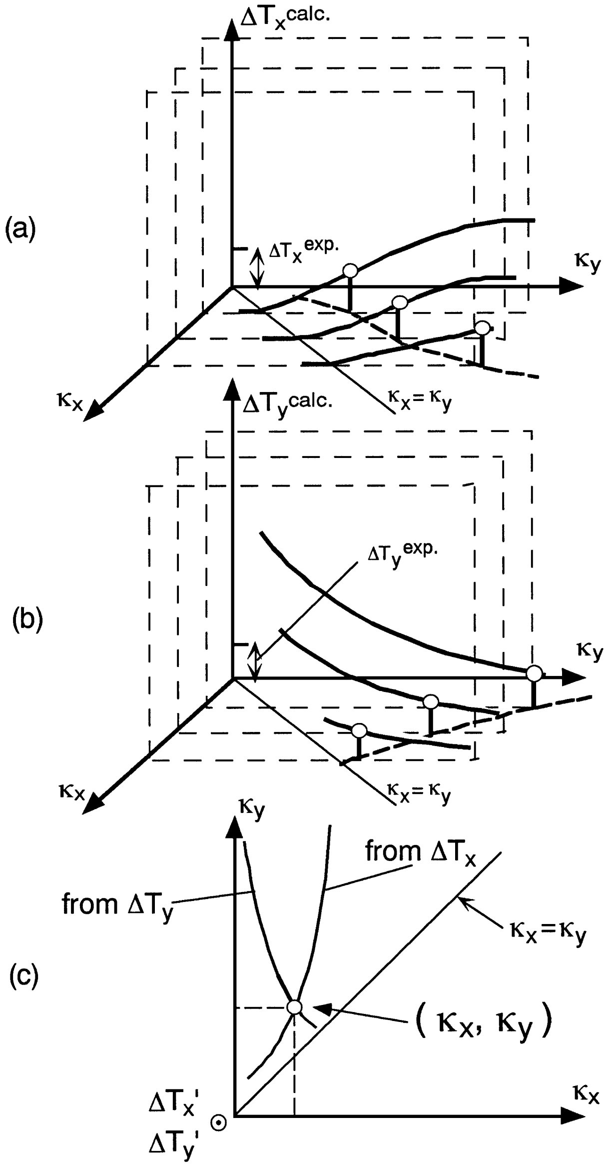

Fig. 5. Conceptional view for determination of the anisotropic thermal conductivities κ_x, κ_y. The calculated temperature differences $\Delta T_x'$ and $\Delta T_y'$ are given for several pairs of the thermal conductivities κ_x, κ_y under a constant applied heat power Q. In (a) and (b), the projections of a set of points to the κ_x-κ_y plane are drawn schematically where $\Delta T_x' = \Delta T_x$ and $\Delta T_y' = \Delta T_y$ are achieved. In (c), a cross-point of the two projection curves can be uniquely obtained and the anisotropic thermal conductivities (κ_x, κ_y) can be decided.

4. Experimental Results and Summary

Figure 6 shows the temperature dependence of the measured values of ΔT_x/Q and ΔT_y/Q for the CFRP sample under the experimental setup shown in Fig. 2. The ΔT_x/Q and ΔT_y/Q (K/mW) values are the temperature differences along the x- and y-directions normalized by the applied heat power Q. The value ΔT_y/Q is larger than ΔT_x/Q over the entire temperature region and increases with decreasing temperature. The ΔT_x/Q values slightly increase as temperature decreases to 50 K and then sharply decrease with further decrease of temperature. In the present experiment, no ΔT_x/Q values could be obtained at $T < 40$ K because the ΔT_x values became very small, which are beneath the detection limit of our system. These results indicate that both κ_x and κ_y values decrease and that anisotropic ratio $A = \kappa_y/\kappa_x$ also decreases with decreasing temperature, as inferred from Fig. 4.

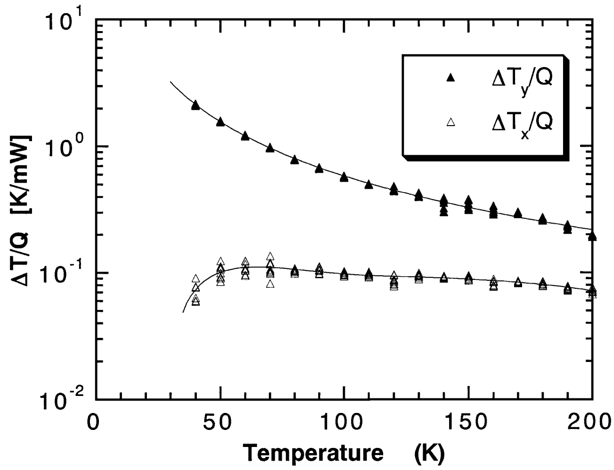

Fig. 6. Temperature dependence of measured ΔT_x/Q and ΔT_y/Q values for the CFRP sample under the experimental setup shown in Fig. 2.

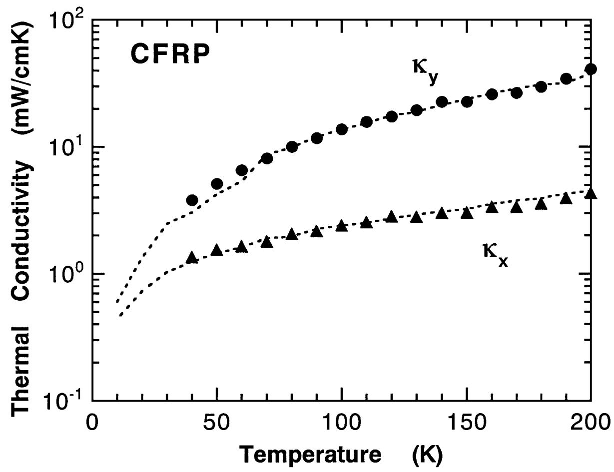

Fig. 7. Thermal conductivities $\kappa_x(T)$, $\kappa_y(T)$ of the CFRP sample as a function of T determined by the present technique. Dashed lines show the thermal conductivities $\kappa_{x0}(T)$, $\kappa_{y0}(T)$ which were measured separately by a 1D steady-state heat flow method using slender rectangular-shaped CFRP samples for each direction.

Figure 7 shows the temperature dependence of the thermal conductivities $\kappa_x(T)$, $\kappa_y(T)$ of the CFRP sample determined by the technique used in this study. In this figure, dashed lines show the thermal conductivities $\kappa_{x0}(T)$, $\kappa_{y0}(T)$ which were measured by the 1D steady-state heat flow method using two slender rectangular-shaped CFRP samples cut from the same bulk sample for each direction. The $\kappa_x(T)$ and $\kappa_y(T)$ values obtained by the present technique are in good agreement with the values measured by the 1D heat flow method. Thus the anisotropic thermal conductivities $\kappa_x(T)$ and $\kappa_y(T)$ can be determined simultaneously and uniquely using a single experimental setup. It is again to be noted that in the present technique, the contact thermal resistivity W_c between the sample and the heater (or the cold finger) does not influence the determination of $\kappa_x(T)$ and $\kappa_y(T)$ because the temperatures at P_1, P_2 and P_3 are directly measured on the sample surface and thus the temperatures at the heater and the cold finger do not appear in the analyses of the heat flow.

In summary, we proposed a new technique for simultaneous determination of the anisotropic thermal conductivities

(κ_x, κ_y) for materials with uniaxial anisotropy using a single experimental setup. This technique can be applied to materials with a wide range of anisotropic thermal conductivity ratios $A = \kappa_y/\kappa_x$ and the various ratios of sample length L_y/L_x. The validity and usefulness of this method were verified using a carbon-fiber-reinforced plastic (CFRP) in the temperature range from 40 K to 200 K.

Acknowledgment

The authors wish to thank T. Kashima and A. Yamanaka of TOYOBO Co., Ltd., in the preparation of the CFRP sample. This work is partially supported by a Grant-in-Aid for Scientific Research from the Ministry of Education, Science, Sports and Culture (No. 09555018).

1) H. Fujishiro, M. Ikebe, K. Noto, M. Matsukawa, T. Sasaoka, K. Nomura, J. Sato and S. Kuma: IEEE Trans. Mag. **30** (1994) 1645.
2) R. Berman: *Thermal Conduction in Solids* (Clarendon Press, Oxford, 1975).
3) S. J. Hagen, Z. Z. Wang and N. P. Ong: Phys. Rev. B **40** (1989) 9389.
4) M. Ikebe, H. Fujishiro, T. Naito and K. Noto: J. Phys. Soc. Jpn. **63** (1994) 3107.
5) J. Crank: *The Mathematics of Diffusion* (Clarendon Press, Oxford, 1975).